Models to Evaluate Flutter Instability of Cable-Suspended Pipelines

Évaluation de l'instabilité de conduites suspendues dues à des oscillations

Modelle zur Bestimmung der Schwingungsinstabilitäten von aufgehängten Pipelines

Giuseppe CREAZZA
Professor
I.U.A.V.
Venice, Italy

Carmelo MAJORANA
Researcher
Universita di Padova
Padua, Italy

Anna SAETTA
Researcher
I.U.A.V.
Venice, Italy

Renato VITALIANI
Associate Professor
Universita di Padova
Padua, Italy

SUMMARY

Flutter instability of cable-suspended pipelines is investigated by means of two different approaches. The first one is based on use of hyper-elastic beams in finite strains, whose motion is governed by non-commutative Lie groups for rotations, parallel transport and exponential mapping. The second one uses eigenvalue analyses of deformed configurations, achieved by means of the finite element method, under both conservative and non-conservative forces and allows to evaluate the instability load for a given structure. The methods are applied to a real test case.

RÉSUMÉ

L'instabilité de conduites suspendues dues à des oscillations est examinée selon deux approches différentes. La première est basée sur l'utilisation de poutres super élastiques avec déformations finies dont le mouvement est régi selon les groupes Lie. La seconde utilise des analyses par valeurs propres des configurations déformées, réalisées au moyen de la méthode des éléments finis, à la fois sous l'action de forces conservatrices ou non; elle permet d'évaluer l'instabilité de charge pour une structure donnée. Les méthodes sont appliquées à des situations réelles et sont comparées.

ZUSAMMENFASSUNG

Die Instabilität der Schwingungen der Kabel, an denen die Pipelines hängen, wird mit zwei verschiedenen Versuchen untersucht. Der Erste basiert auf dem Gebrauch von hyperelastischen Trägern mit massiger Spannung, deren Bewegungen von einer nicht kommutativen Lie-Gruppe für Rotationen, parallelem Transport und eine Exponentialkarte geleitet wird. Der Zweite benutzt Eigenwertbetrachtungen von verformten Strukturen, ausgeführt durch die Methode der finiten Elemente unter konservativen, sowohl nicht konservativen Kräften, und erlaubt die Bestimmung der unstabilen Last für eine gegebene Konstruktion. Die Methoden sind an einem reellen Fall angewendet.

1. INTRODUCTION

Cable suspension pipelines subjected to wind loads can suffer flutter instability. Turbulence phenomena may rise around suspension pipelines with mechanisms like the Von Karman's one. Hence a corresponding structural evaluation is needed for this purpose. In literature such a study is performed by means of eigenvalue analyses since coincidence of exciting force frequency with one or more natural frequencies gives rise to resonance phenomena [e.g. 1,2]. In this paper, an investigation of instability phenomena of suspension pipelines is proposed by means of two different procedures. The first procedure is based on the use of a geometrically exact approach to analyse deformable beams in large motions [3,4,5]. Main features of the formulation are the SO(3) noncommutative Lie group employed to follow the rotation of the beam transverse section and the concepts of exponential mapping and parallel transport for numerical integration of the involved equations. Hence elastic instability problems like flutter are treated in a natural way, achieving exact consistent linearized results with quadratic rate of convergence. The second procedure is based on a nonlinear finite element analysis of elastic structures subjected to conservative as well as nonconservative forces [6,7,8]. The stability of the structural system is checked by means of eigenvalue analyses of the deformed configurations. Modes of instability, flutter and divergence, together with values of critical loads are identified both in presence and in absence of damping. This approach appears direct and effective. It is also usefull if compared with general purpose F.E. codes, since nonconservative forces coupled with eigenvalue analysis are not included in usual nonlinear dynamic analyzers. Comparisons between the two approaches are carried out as evaluation procedures to determine the structural performances. The case of a real cable suspension pipeline [2] is considered as example.

2. MATHEMATICAL APPROACHES

2.1 First method.

The analysis is carried out within a general approach, based on the beam model due to J.C. Simo [3,4,5]. This allows to investigate the mechanical behaviour of structural elements in the framework of large strains, displacements and rotations. Moreover, the wide application spectrum of the stated mathematical approach allows to analyse in this context any problem involving elastic stability or non conservative loads. The effect of finite rotations is analysed within the orthogonal SO(3) Lie group. The formulation incorporates as essential concepts those of exponential mapping (for the configuration update) and of parallel transport. The theory can be applied both in analytical form, for calibration purposes, and in a discrete one by means of finite element technique. In the latter case, the update is performed exactly, since Rodrigues' formula is applied to update rotations. After posing the equilibrium in functional form, linearization procedures are employed, leading to geometrical and material tangent stiffnesses. Consequently quadratic convergent rates are achieved within a solution alghoritm of Newton-Raphson type, allowing efficient analysis of a wide range of problems, like finite vibration or dynamic stability and motions implying finite displacements and rotations of flexible beams. In the following a brief account of the governing equations is given.

2.1.1 Reference systems. Kinematic assumptions.

The actual configuration of the beam is described introducing the following objects:

1. A curve defined within an open interval $\Sigma \subset R$, $S \in I \rightarrow \varphi_0(S) \in R^3$, called centre line.
2. A family of planes defined by the unit vector field, $S \in I \rightarrow \mathbf{n}(S) \in R^3$. Planes through $\varphi_0(S)$ orthogonal to $\mathbf{n}(S)$, $S \in \mathbf{I}$, are defined as beam sections.
3. A fiber inside each section defined by the unit vector field, $S \in I \rightarrow \mathbf{t}_I(S) \in R^3 \quad I = 1,2.$
   As a consequence, each point of the curve $S \rightarrow \varphi_0(S)$ can be associated to an orthogonal reference system $\{\mathbf{t}_1(S), \mathbf{t}_2(S), \mathbf{n}(S)\}$, called the intrinsic or convected system.

2.1.2 Exponential map

The rotations $\theta \in so(3)$ (space of emisymmetric tensors) are treated by means of the explicit Rodrigues formula:

$$\exp[\theta] = 1 + \frac{\sin\|\theta\|}{\|\theta\|}\theta + \frac{1}{2}\frac{\sin^2(\|\theta\|/2)}{(\|\theta\|/2)^2}\theta^2 \tag{1}$$

which allows the exact updating of the rotation tensor pertaining to a given transverse section of the beam. The above formula is fundamental with respect to the next developments.

2.1.3 Forces and couples. Equations of motion.

Given a section $A_t = \varphi_t\big|_{s=fixed}(A)$ in the current configuration and defining $\mathbf{P}(\xi,t)$ as the first Piola-Kirchhoff stress tensor, a two-point tensor given by

$$\mathbf{P}(\xi,s) \equiv \mathbf{T}_1(\xi,s)\otimes\mathbf{E}_1 + \mathbf{T}_2(\xi,s)\otimes\mathbf{E}_2 + \mathbf{T}_3(\xi,s)\otimes\mathbf{E}_3 \tag{2}$$

with $\mathbf{T}_3(S,\xi) = \mathbf{P}(S,\xi)\mathbf{E}_3$ the stress vector acting on the section $\mathbf{A} \subset \mathbf{R}^2$, the resultant contact force by unit reference arc-length $\mathbf{n}(S,t)$ on the section A_t of the current configuration is given by

$$\mathbf{n}(\xi,S) \equiv \int_A \mathbf{P}(\xi,S)\mathbf{E}_3 d\xi = \int_A \mathbf{T}_3(\xi,S)d\xi \quad , \tag{3}$$

and similarly the resultant couple by unit reference arc-length $\mathbf{m}(S,t)$ on the section A_t of the actual configuration is represented by

$$\mathbf{m}(S,t) = \int_A [\mathbf{x} - \varphi_0(S,t)]\times\mathbf{T}_3(\xi,S)d\xi \,. \tag{4}$$

2.1.4 Internal energy. Strain measures.

The internal energy, in terms of spatial forces and moments $\mathbf{n}(S,t)$ and $\mathbf{m}(S,t)$ takes the form [4]:

$$\Pi \equiv \int_{A\times I} \mathbf{P} : \mathbf{F}d\xi dS = \int_I (\mathbf{n}\cdot\tilde{\gamma} + \mathbf{m}\cdot\tilde{\omega})dS \tag{5}$$

where $\tilde{\omega}(S,t)$ is the spatial vector related to the curvature, $\tilde{\gamma}(S,t)$ is the spatial strain vector:

$$\tilde{\gamma}(S,t) \equiv \frac{\partial\varphi_0}{\partial S}(S,t) - \mathbf{n}(S,t). \tag{6}$$

$\Psi(\Gamma,\kappa)$ is the properly invariant internal energy function, which can be represented in the material form as

$$\Psi(\Gamma,\kappa) = \frac{1}{2}[\Gamma_t,\kappa_t]\,\mathrm{Diag}[GA_1, GA_2, EA, EI_1, EI_2, GJ]\begin{Bmatrix}\Gamma\\ \kappa\end{Bmatrix} \tag{7}$$

with Γ and κ the material forms of the linear and angular deformations.

2.1.5 Weak form. Inertia operator.

Given $\varphi=(\varphi_o,\Lambda)\in C$, the current configuration and $\eta \equiv (\eta_0,\psi)$, a kinematic admissible variation in the spatial reference, with $\eta\in T_\varphi C$, multiplying the spatial form of the local equilibrium equations reported in Table I, times an arbitrary admissible variation η the nonlinear functional is obtained

$$G_{dyn}(\varphi,\eta) := \int_0^L \left\{A_\rho\ddot{\varphi}_0\cdot\eta_0 + \left[I_\rho w + w\times(I_\rho w)\right]\psi\right\}dS + G(\varphi,\eta) = 0 \tag{8}$$

where $G(\varphi,\eta)$ represents the weak form of the local static equilibrium equations,

$$G(\varphi,\eta) := \int_{[0,L]}\left\{\frac{\partial\psi(S,\Gamma,\Omega)}{\partial\Gamma}\cdot\Lambda^t\left[\frac{\partial\eta_0}{\partial S} - \psi\times\frac{\partial\varphi_0}{\partial S}\right] + \frac{\partial\psi(S,\Gamma,\Omega)}{\partial\Omega}\cdot\Lambda^t\frac{\partial\psi}{\partial S}\right\}dS - \int_{[0,L]}(\mathbf{n}\cdot\eta + \mathbf{m}\cdot\psi)dS\,, \tag{9}$$

with respect to an arbitrary $(\eta_0,\psi\Lambda)\in T_\varphi C$. Homogeneous boundary conditions (Dirichlet's conditions) are chosen as example.

(1) **Material** deformations and **spatial** stresses

$$\Gamma = \Lambda^{t}\frac{\partial \varphi_0(S,t)}{\partial S} - \mathbf{E}_3, \qquad \Omega = \Lambda^{t}\omega, \qquad \mathbf{n} = \Lambda\frac{\partial \psi(S,\Gamma,\Omega)}{\partial \Gamma}, \qquad \mathbf{m} = \Lambda\frac{\partial \psi(S,\Gamma,\Omega)}{\partial \Omega}. \tag{10a,b,c,d}$$

(2) **Spatial** local linear and angular equilibrium

$$\frac{\partial \boldsymbol{n}}{\partial S} + \tilde{\boldsymbol{n}} = A_\rho \ddot{\varphi}_0 \qquad \frac{\partial \mathbf{m}}{\partial S} + \frac{\partial \varphi_0}{\partial S} \times \mathbf{n} + \mathbf{m} = \mathbf{I}_\rho \mathbf{w} + \mathbf{w} \times \left[\mathbf{I}_\rho \mathbf{w}\right] \tag{11a,b}$$

Table I

2.1.6 Tangent stiffnes

The consistent linearization of the weak form allows to find the tangent stiffness matrix defined as:

$$\boldsymbol{K}_{IJ}\left(\Lambda_n, \varphi_{n+1}^{(i)}\right) = \boldsymbol{M}_{IJ}\left(\Lambda_n, \Lambda_{n+1}^{(i)}\right) + \boldsymbol{S}_{IJ}\left(\varphi_{n+1}^{(i)}\right) + \boldsymbol{G}_{IJ}\left(\Lambda_{n+1}^{(i)}\right) + \boldsymbol{L}_{IJ}\left(\Lambda_{n+1}^{(i)}\right) \tag{12}$$

The discrete tangent dynamic operator $\kappa_{IJ}(\Lambda_n, \varphi_{n+1}^{(i)})$ coupling the degrees of freedom of node I with those of node J is the assembling of the following tangent matrices: i) the inertia matrix, ii) the material stiffness matrix, iii) the geometric stiffness matrix, iv) the matrix due to follower forces. The application of eq. (12) to stability problems in presence of follower forces can be found in [5].

2.2 Second approach

2.2.1 Finite element formulation

Within a Total Lagrangian approach, the Green's strains and the Piola Kirchhoff's stresses are used to approximate the non linear 3D beam element presented in [7]. By using the theory of geometrically nonlinear analysis within the classical finite element method, the global stiffness matrix $\boldsymbol{K}_T$ of the structure can be written as in eq. (12), by the addition of the Cartesian elastic, the initial displacement and the initial stress stiffness matrices: $\boldsymbol{K}^0$, $\boldsymbol{K}^L$ and $\boldsymbol{K}^S$ respectively. Nonconservative forces of the follower type lead to non-self-adjoint boundary value problems. Within the finite element formulation, the effect of such forces is in fact to produce a non-symmetric load correction matrix $\boldsymbol{K}^{nc}$ which has to be added to the total tangent stiffness matrix [6,7,8]. Therefore the total tangent matrix becomes non-symmetric and can be expressed by:

$$\mathbf{K}_T = \mathbf{K}^0 + \mathbf{K}^L + \mathbf{K}^S - \mathbf{K}^{nc} \tag{13}$$

2.2.2 Problem of elastic stability

The tangential equation of motion in the finite element formulation can be written as follows:

$$\boldsymbol{M}\ddot{\boldsymbol{u}} + \boldsymbol{C}_T\dot{\boldsymbol{u}} + \boldsymbol{K}_T\boldsymbol{u} = \boldsymbol{0} \tag{14}$$

where $\boldsymbol{M}$, $\boldsymbol{C}_T$, and $\boldsymbol{K}_T$ are respectively the global mass matrix, the tangential damping matrix and the tangential stiffness matrix, $\boldsymbol{u}$ is the displacement vector. The eigenvalue problem related to eq. (14), transformed by using the phase space is the following one [7]:

$$\left(\begin{bmatrix}\mathbf{M} & \mathbf{0}\\ \mathbf{0} & \mathbf{K}_T\end{bmatrix} - \lambda\begin{bmatrix}\mathbf{0} & \mathbf{M}\\ -\mathbf{M} & -\mathbf{C}_T\end{bmatrix}\right)\begin{bmatrix}\lambda\mathbf{u}_0\\ \mathbf{u}_0\end{bmatrix} = 0 \tag{15}$$

Eq. (15), assuming regularity and positive definiteness for the mass matrix ($detM \geq 0$ and $M > 0$), becomes:

$$\mathbf{A}_T\mathbf{X}_0 = \lambda\mathbf{X}_0 \qquad \text{where} \qquad \mathbf{A}_T = \begin{bmatrix}-\mathbf{M}^{-1}\mathbf{C}_T & -\mathbf{M}^{-1}\mathbf{K}_T\\ \mathbf{I} & \mathbf{0}\end{bmatrix} \tag{16}$$

The stability behaviour of systems governed by equation (14) can be studied by examining the nature of the eigenvalues of the problem, in the neighbourhood of the current equilibrium solution. Therefore the eigenvalues λ_k of (16a) at each load step have to be computed by means of a

numerical procedure for unsymmetric matrices and the stability conditions [7] become: a)if all $Re(\lambda_k) = \alpha_k$ are negative, the position is asymptotically stable; if at least one $Re(\lambda_k) > 0$ exists, the position is unstable; If some eigenvalues have negative real parts, while the others have zero real parts, the position is weakly stable.

These are the stability assessments of Ljapunov, where the real part of the characteristic exponents are the well-known Ljapunov exponents. Moreover, the *divergence critical load* occurs when at least one eigenvalue λ_{ki} vanishes and the conjugate λ_{kj} becomes negative real, while the remaining eigenvalues are complex conjugate with negative real parts. If the load slightly increases over the critical load, the zero eigenvalue becomes one, with positive real parts, showing that the trivial state becomes locally unstable. The *flutter critical load* occurs when at least one pair of eigenvalues λ_k become pure imaginary eigenvalues, while the remaining eigenvalues are complex conjugate with negative real parts. If the load slightly increases over the critical load, the zero real parts of the pure imaginary eigenvalues become positive, showing that the trivial state is locally unstable and also that there is an oscillatory motion with increasing amplitude.

For undamped systems, usually the stability behaviour is studied by considering the square of the eigenfrequencies of the system, defined as $\omega^2 = -\lambda^2$. Therefore the divergence critical load is the value of the load to which the smallest square of the eigenfrequencies becomes equal to zero, while the flutter critical load is the value of load to which the two smallest eigenvalues approach each other until they coalesce.

3. NUMERICAL EXAMPLE

Some preliminary investigations with the proposed procedures are carried out, with reference to the case of a cable suspension pipeline. Using the first approach, stability diagrams are built-up to show stability conditions under exciting wind load. Moreover the values of the critical loads are found by means of the second approach. The geometric configuration is shown in Fig. 1. It is taken from Ref. [2], where the case was originally investigated, finding the first eigenfrequencies and eigenmodes. A symply supported tube-beam of circular cross section is considered for this purpose, together with a suspension cable of parabolic shape, connected to the former with vertical rods. Four lenghts are taken into account for the beam, from 50 m to 200 m with maximum height to span ratio of 1/6, 1/8, 1/10. The investigated outer diameters are 250, 400 and 560 mm, with thicknesses of 10, 10.3, 11.9 mm, respectively. The Young's modulus of the material used is equal to 160 Gpa. Periodic wind actions are applied, which have the well known self-exciting character. The research is here limited, as example, to the first resonance fequency. According to the beam motion, see Ref. [2], the load has a "following" character. For comparison, also the case of "non-following" forces has been taken into account. With the above indicated procedure, it was possible to find the stability diagrams of the cable suspended pipeline, as function of the span, height to span ratio, tube diameters and thicknesses. As usually, the diagrams are represented in non-dimensional form. As a results of the analyses, it was found that the boundaries of the principal regions of instability in nondimensional representation appears quite similar for the investigated cases. One of them is reported in Fig. 2 as example. In this representation, the ratio of the amplitude of the periodic load to the critical load is reported in the abscissa and the ratio of the exciting frequency to the first natural frequency is reported as ordinate. It can be observed the norrowing effect of the follower forces with respect to the unstable region. The values of the critical load found with the second approach are in agreement with those predicted in Ref. [2].

4. CONCLUSIONS

As a conclusion, it can be stated that the computational approaches here presented allow to gain a thorough understanding of the nonlinear geometrically behaviour of complex systems like the one taken into account in this paper. The research will be extended to include viscous damping effects.

REFERENCES

1. Creazza G., Mele M. (eds.), *Advanced problems in bridge construction,* CISM courses, 1991
2. Vitaliani R., Self-excited vibrations of cable suspension pipelines under constant wind loads, *C.T.A. Conference,* october 1977, (in italian).
3. Simo J.C., A finite strain beam. Part I, *Comput. Meths. Appl. Mech. Engrg,* 1985, 55-70
4. Simo J.C., Vu-Quoc L., Three-dimensional finite strain rod model. Part II:Computational aspects, *Comput. Meths. Appl. Mech. Engrg.*, 1986, 79-116
5. Simo J.C., Vu-Quoc L., On the dynamics in space of rods undergoing large motions- a geometrically exact approach, *Comput. Meths. Appl. Mech. Engrg.*, 1988, 125-161
6. Argyris, J.H, Symeondis, S., Nonlinear finite element analysis of elastic systems under nonconservative loading. Natural formulation. Part I Quasistatic problem, *Comput. Methods Appl. Mech. Engrg.* **26**, 1981, 75-123.
7. Gasparini, A., Saetta, A., Vitaliani, R. On the stability and instability regions of nonconservative continuous system under partially follower forces, in press, *Comput. Meths. Appl. Mech. Engrg.*
8. Zienkiewicz O. C., Taylor R. L., *The Finite Element Method,* vol I-II, McGraw-Hill, 1989.

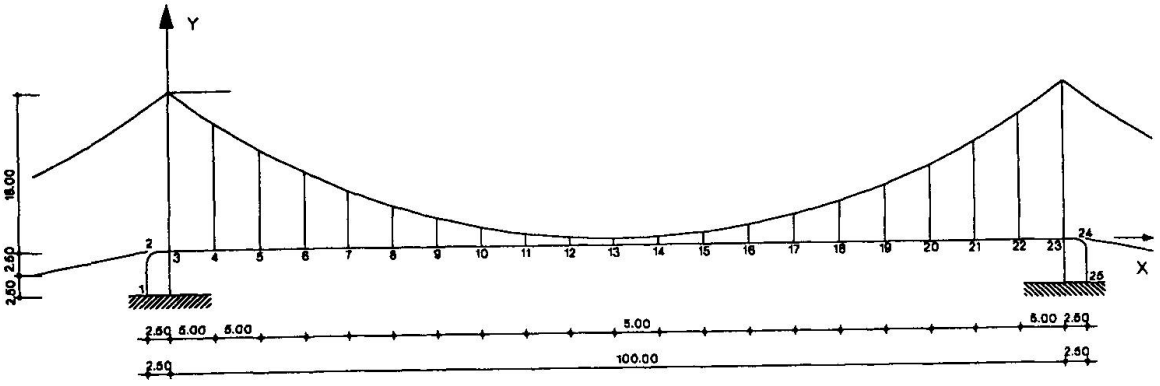

Fig. 1 - Model problem

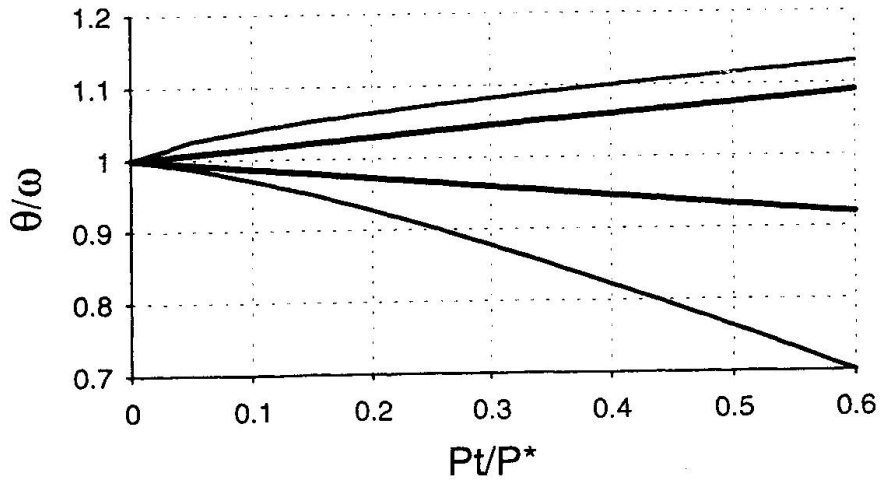

Fig. 2 - Stability diagram (bold line: follower forces)